Phase Behavior, Densities, and Isothermal Compressibility of CO_2 + γ-Valerolactone Systems in Various Phase Regions

Yucui Hou,[†,‡] Weize Wu,*[,†] and Martyn Poliakoff*[,§]

State Key Laboratory of Chemical Resource Engineering, College of Chemical Engineering, Beijing University of Chemical Technology, Beijing 100029, China, School of Chemistry, University of Nottingham, Nottingham NG7 2RD, U.K., and Taiyuan Normal University, Taiyuan 030012, China

The phase behavior of CO_2 and γ-valerolactone (GVL) has been measured using a high-pressure variable-volume view cell and a fiber optic reflectometer. The density of the binary mixture has also been measured, and the isothermal compressibility (K_T) of the binary mixture was calculated from the density of the binary mixture. The phase transition points, bubble point, dew point, and critical point, have been measured on the range of GVL mole fraction from 0.01 to 0.15 and temperatures from (308.2 to 550.2) K. The density of the mixture is sensitive to the pressure near the critical point of the mixtures, and K_T is also sensitive to the pressure when the pressure is close to the phase transition point, especially close to the critical point. When the pressure is much higher than the phase separation pressure or the composition is far from the critical composition, K_T is very small and the effect of pressure on K_T is very limited. The phase boundary data of the binary mixture can be correlated well by the Peng−Robinson equation of state (PR EOS) with two interaction parameters.

Introduction

γ-Valerolactone (GVL) has low melting (−31 °C), high boiling (207 °C), and open cup flash (96 °C) points, has a definitive but acceptable smell for easy recognition of leaks and spills, and is miscible with water, assisting biodegradation. GVL can be synthesized from renewable biomass. So GVL is renewable, easy, and safe to store and move globally in large quantities. Therefore, GVL could be considered as a sustainable liquid for global storage/transportation and a renewable hydrocarbon resource for energy and carbon-based consumer products.[1]

Although GVL is a renewable hydrocarbon resource, traditionally the process of GVL synthesis is not environmentally benign because the process used many harmful or corrosive solvents, such as strong acid[2] and dioxane.[3]

In recent years, scientists and engineers have paid much attention to supercritical fluids (SCFs). Some are attracted by the unusual properties of the SCFs, while others are more interested in the applications of this kind of fluids. Carbon dioxide is one of the more popular solvents because it is nontoxic, nonflammable, inexpensive, readily available in large quantities, and has moderate critical temperature and pressure (304.3 K and 7.38 MPa). So supercritical CO_2 is recognized as an environmentally benign solvent, and it has been widely used as the solvent in supercritical fluid extraction and chemical reactions.

Recently, Poliakoff et al.[4] and Manzer et al.[5] reported that hydrogenation of levulinic acid can produce GVL in supercritical CO_2. Therefore, GVL can be synthesized in supercritical CO_2 or be separated from the mixture of products using supercritical CO_2 for saving energy and protecting the environment. As we know, the phase behavior and critical parameters of fluid systems can be crucial for different chemical processes. Measurement of this behavior has been an interesting topic for years, and many related papers have been published, including the study of various mixtures.

However, as far as we are aware, no paper has reported the phase behavior of CO_2 + GVL at elevated pressures. In this study, we have determined the phase behavior and critical parameters of the CO_2 and GVL system, and the densities of CO_2 and GVL at different conditions were also measured. The compressibility of the mixture was then studied systematically in different phase regions, and the effect of the phase behavior on the density and isothermal compressibility were also investigated, especially in the critical region. The measured phase boundary data of the system are modeled using the Peng−Robinson equation of state (PR EOS).

Experimental Section

Materials. CO_2 (99.995 %) used in Beijing was purchased from the Beijing Haipu Company, and CO_2 (99.95 %) used in Nottingham was purchased from CryoServise. CO_2 was used as received. GVL (> 98 %) used in Beijing was analytical grade produced by the Beijing Chemical Reagent Plant, which was distilled before used, and GVL (> 98 %) used in Nottingham was also analytical grade produced by Alfa Aesar, which was used as received.

Apparatus and Procedures of the Static Method. The phase behavior and the densities of the mixtures were determined using a high-pressure variable-volume view cell, and the apparatus and procedures were similar to those used in the previous papers.[6,7] The constant-temperature water bath was controlled by a temperature controller, and the temperature was monitored by high-precision mercury thermometers with an accuracy of

* Authors to whom correspondence should be addressed. E-mail: wzwu@mail.buct.edu.cn. Tel.: +86 10 64427603. Fax: +86 10 64421073. E-mail: martyn.poliakoff@nottingham.ac.uk. Tel.: +44 115 951 3520. Fax: +44 115 951 3058.
[†] Beijing University of Chemical Technology.
[‡] Taiyuan Normal University.
[§] University of Nottingham.

10.1021/je8007759 CCC: $40.75
Published on Web 12/12/2008

better than ± 0.05 K. The pressure was determined by a pressure transducer and an indicator (Beijing Tianchen Instrument Company) with an accuracy of ± 0.025 MPa in the range of (0 to 20) MPa, calibrated with a Heise Standard pressure gauge.

In a typical experiment, the apparatus was washed thoroughly using different solvents and dried under a vacuum. A known mass of GVL was charged first using a syringe, then the air in the system was flushed with CO_2. CO_2 was then added using a sample bomb. The mass of the chemicals in the system was calculated from the mass difference of the sample bomb before and after charging the system. The cell was placed into the water bath at the desired temperature. After thermal equilibration, the piston in the view cell was moved up and down to change the volume and the pressure of the system, and the phase separation could be observed directly. At the critical point, very strong opalescence was observed, and the meniscus appeared at half-volume after a slight pressure reduction. The volume of the system was known from the position of the piston, which was calibrated accurately using water as a medium. The composition and density of the mixture could easily be calculated from the masses of the components and the volume of the system.

It is estimated that the accuracy of the density data is accurate to ± 0.002 $g \cdot cm^{-3}$, the accuracy of the bubble point pressure, critical pressure, and dew point pressure is better than ± 0.05 MPa, and that of the bubble point temperature, critical temperature, and dew point temperature is better than ± 0.1 K. To calculate the compressibility (K_T), we used a B-spline method to smooth the measured density data, and K_T was obtained by differential calculation. It was estimated that the accuracy of the K_T data was better than ± 3 %.

Apparatus and Procedures of Fiber Optic Reflectometer (FOR). The phase behavior of CO_2 and GVL at higher temperatures was measured at the University of Nottingham. The apparatus and procedures have been reported in detail in our previous papers.[8,9] In brief, the apparatus consists of a CO_2 cylinder, two high-pressure reciprocating pumps (Gilson, 308), a 1.5 mL dynamic mixer (Gilson 811C), a preheater (an 8 m coil of 1/16″ o.d. tubing), an equilibrium cell, a GC oven-controlled air bath, a back pressure regulator (BPR) (JASCO 880-81), an optic sensor, a pressure gauge, and a temperature indicator. The reciprocating pumps were used to keep a constant flow rate when the system pressure was varied.

In a typical experiment, CO_2 and organic solvent were pumped at a fixed ratio into the equilibrium cell via the mixer and preheater. First, the temperarure and pressure are controlled until a single phase is formed in the equilibrium cell. When equilibrium is reached, the signal of the FOR monitored, as monitored on a PC, becomes constant with time. Then, conditions can be slowly changed to reach a phase transition point, either by changing the pressure with the BPR or by changing the temperature via the temperature controller. When the phase transition is reached, there is an obvious jump on the signal of the FOR.[9]

Results and Discussion

Critical Points and Phase Behavior of the Mixtures. Table 1 summarizes the bubble point, critical point, and dew point temperatures and pressures for the binary system at different compositions, with the mole fraction of GVL varying from 0.01 to 0.15. The critical point is located between bubble point and dew point if there is no critical point shown at the composition. Figure 1 gives a graphical representation of the experimentally determined phase boundaries. There is a two-phase region below or inside the lines of fixed composition, while the one phase region is above or outside of these lines. We used two methods to measure the phase boundary of the binary system, FOR, and a high-pressure variable-volume view cell. The data from the two methods show a good agreement.

Table 1. Experimental Bubble Points, Critical Points, and Dew Points of CO_2 (1) + GVL (2) at Fixed Molar Compositions

T/K	p/MPa	phase transition[a]		T/K	p/MPa	phase transition[a]	
			$x_2 = 0.010$				
308.2	7.62	b	s	353.2	13.57	d	f
313.2	8.29	b	s	373.2	14.86	d	f
318.0	9.04	d	s	393.2	13.94	d	f
322.9	9.83	d	s	403.2	12.58	d	f
323.2	9.83	d	f	413.2	11.03	d	f
327.9	10.55	d	s	423.2	9.52	d	f
332.9	11.31	d	s	430.2	6.48	d	f
333.2	10.94	d	f				
			$x_2 = 0.025$				
308.2	7.58	b	s	373.2	16.78	d	f
313.2	8.34	b	s	393.2	18.60	d	f
316.2	8.73	cp	s	423.2	19.69	d	f
318.0	9.18	d	s	433.2	19.23	d	f
322.9	10.22	d	s	443.2	18.18	d	f
323.2	10.62	d	f	453.2	16.66	d	f
327.9	11.27	d	s	460.4	14.48	d	f
332.8	12.26	d	s	463.0	12.44	d	f
333.2	12.75	d	f	468.7	10.40	d	f
343.2	13.69	d	f	462.1	7.21	d	f
353.2	15.10	d	f				
			$x_2 = 0.050$				
308.2	7.50	b	s	413.2	23.33	d	f
313.2	8.30	b	s	433.2	24.25	d	f
318.0	9.25	cp	s	453.2	23.70	d	f
322.9	10.46	d	s	463.2	22.75	d	f
323.2	10.78	d	f	473.2	21.37	d	f
327.9	11.62	d	s	483.2	19.95	d	f
332.9	12.81	d	s	493.2	17.91	d	f
333.2	12.98	d	f	498.2	15.34	d	f
343.2	15.08	d	f	500.2	12.88	d	f
353.2	16.68	d	f	503.2	10.58	d	f
373.2	19.54	d	f	501.2	9.02	d	f
393.2	21.91	d	f	500.2	7.18	d	f
			$x_2 = 0.100$				
308.2	7.43	b	s	393.2	24.12	d	f
313.2	8.27	b	s	413.2	25.91	d	f
318.0	9.28	b	s	433.2	27.21	d	f
322.9	10.52	b	s	453.2	27.85	d	f
327.9	11.73	b	s	473.2	27.73	d	f
332.9	13.01	b	s	493.2	26.49	d	f
333.2	13.45	b	f	513.2	24.10	d	f
337.9	14.23	cp	s	530.2	20.68	d	f
343.2	15.65	d	f	543.2	17.24	d	f
353.2	17.80	d	f	549.2	13.79	d	f
363.2	19.66	d	f	550.2	11.00	d	f
373.2	21.29	d	f	545.2	9.00	d	f
383.2	22.82	d	f	543.2	7.21	d	f
			$x_2 = 0.150$				
308.2	7.25	b	s	373.2	21.51	b	f
313.2	8.12	b	s	393.2	24.41	b	f
318.0	9.04	b	s	413.2	26.62	d	f
322.9	10.10	b	s	433.2	28.24	d	f
323.2	10.64	b	f	453.2	29.00	d	f
327.8	11.33	b	s	473.2	29.28	d	f
332.9	12.56	b	s	493.2	28.81	d	f
333.2	13.22	b	f	513.2	27.69	d	f
343.2	15.62	b	f	533.2	25.83	d	f
353.2	17.75	b	f				

[a] b: bubble point; cp: critical point; d: dew point. [s]: data measured via volume-variable view cell. [f]: data measured via FOR.

Density and Isothermal Compressibility. The densities of the mixture at temperatures up to 338 K and at different pressures were measured using the high-pressure variable-volume view cell. The data determined at different conditions are listed in

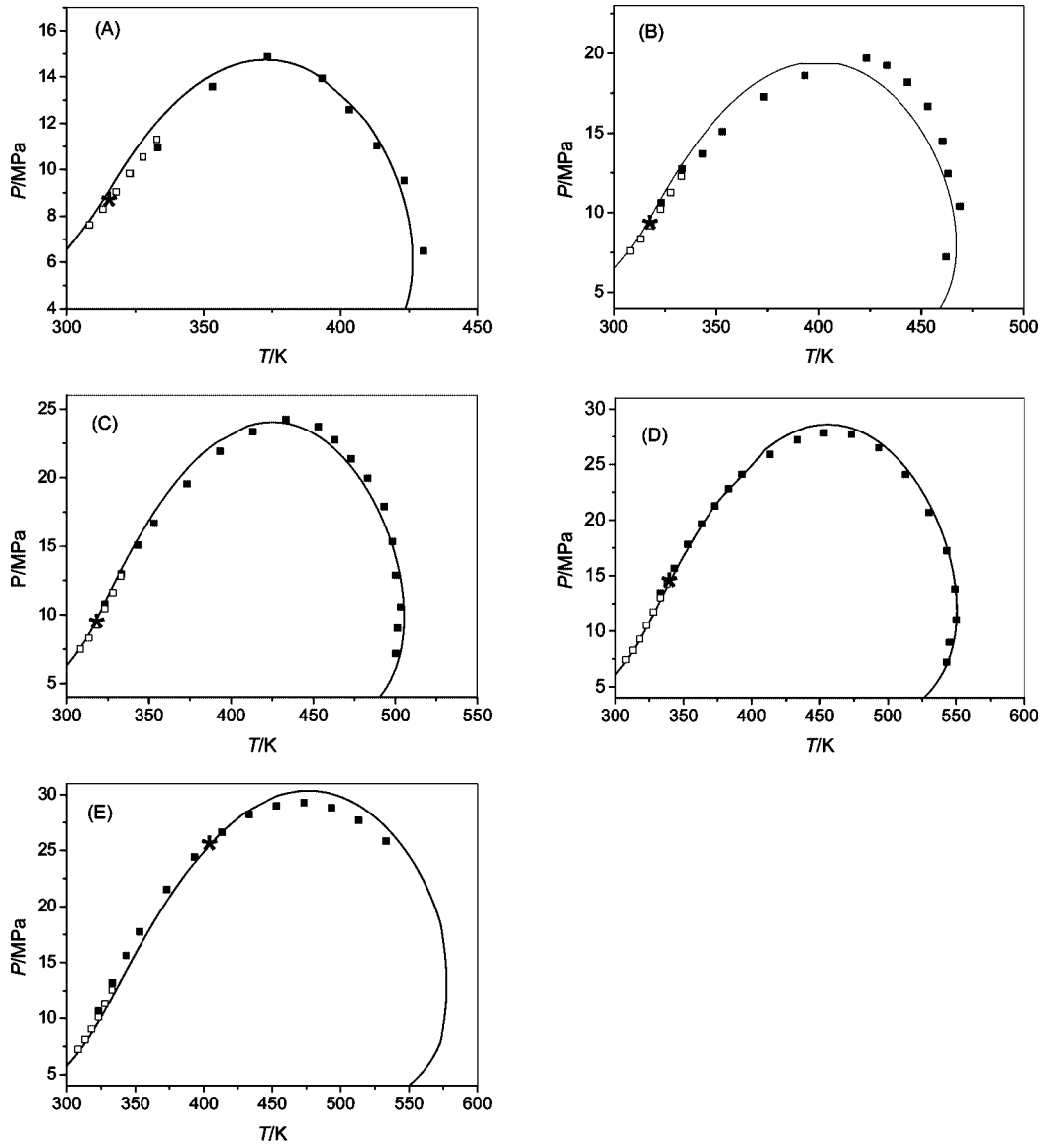

Figure 1. Phase boundary of CO_2 (1) and GVL (2) with different compositions: (A), $x_2 = 0.010$; (B), $x_2 = 0.025$; (C), $x_2 = 0.050$; (D), $x_2 = 0.100$; (E), $x_2 = 0.150$. Experimental data (in symbols) obtained by ■, FOR; and □, the view cell and calculated results by the PR−EOS (in lines). Critical points (*) measured or estimated by dew and bubble points are also indicated.

Table 2. Figure 2 illustrates the dependence of the density of the binary mixtures on pressure and temperature. It can be seen from Figure 2 that a similar tendency was observed for different compositions. Obviously at fixed composition and fixed temperature, the density increases with increasing pressure, and at fixed composition and fixed pressure, the density decreases with increasing temperature. When the concentration of GVL increases, the density also increases, which is probably because the molecular weight of GVL is greater than that of CO_2.

At pressures close to the phase boundary, especially near the critical point, the density of the mixture changes greatly. For example, when the concentration of GVL is 0.025 in mole fraction, the critical temperature is 316.2 K and the critical pressure is 9.25 MPa. The density of the mixture decreases greatly when the pressure is decreased close to the critical point. However, when the pressure is far away from the phase boundary, the density has no obvious change.

The results in Figure 2 demonstrate that the sensitivity of density to pressure depends on both the composition and the pressure at a fixed temperature. The isothermal compressibility (K_T) of a fluid is a quantitative expression of the sensitivity of density to pressure, which is closely related with the structure of fluids.[10] K_T values of the mixture can be calculated by the following equation

$$K_T = \frac{1}{\rho}\left(\frac{\partial \rho}{\partial P}\right)_T \tag{1}$$

where ρ is the density of fluid and P is the pressure.

Figure 3 shows the effect of the pressure on K_T for mixtures of different compositions. As can be seen from the figures, K_T is large and sensitive to the pressure as the pressure approaches the critical point of a mixture; that is, K_T increases sharply as the pressure approaches the critical pressure. It also can be seen that K_T increases significantly as the pressure approaches the values at the dew and bubble points. However, K_T is very small and not sensitive to the pressure when the pressure is far away from the phase separation pressure.

The data in Figure 3 also illustrate that when the temperature is far from the critical temperature the effect of pressure on K_T is limited, even near the phase separation point, especially in Figure 3d and 3e.

Correlation. The Peng−Robinson equation of state[11] (PR EOS) was used to correlate the vapor−liquid equilibrium data and the critical points of the mixtures. The PR EOS and the mixing rules used are shown as follows.

$$P = \frac{RT}{v-b} - \frac{a}{v(v+b)+b(v-b)} \quad (2)$$

The constants a and b can be obtained from the related parameters of pure components using the following equation.[11]

$$a = 0.457235\frac{R^2T_c^2}{P_c}\alpha \quad (3)$$

$$b = 0.077796\frac{RT_c}{P_c} \quad (4)$$

$$\alpha = [1 + m(1-\sqrt{T/T_c})]^2 \quad (5)$$

$$m = 0.37464 + 1.54266\omega - 0.26922\omega^2 \quad (6)$$

For a mixture, the van der Waals mixing rules are applied[11]

$$a = \sum_i \sum_j x_i x_j \sqrt{a_i b_j}(1-k_{ij}) \quad (7)$$

$$b = \sum_i \sum_j 0.5 x_i x_j (b_i + b_j)(1-l_{ij}) \quad (8)$$

where T_c, P_c, and ω stand for critical temperature, critical pressure, and acentric factor; a_i and b_i are parameters of pure components; k_{ij} and l_{ij} are the binary interaction parameters for the (i, j) pair; and x_i is the mole fraction of the ith component.

The physical property information (T_c, P_c, and ω) used for the pure component CO_2 is taken from NIST (see Table 3). GVL physical properties were calculated using the method reported by Joback and Reid;[12] the results are also listed in Table 3.

Binary interaction parameters are empirical parameters that can be regressed from the binary data by minimizing the average absolute deviation for bubble and dew point pressures. A single interaction parameter can usually be used to calculate the phase behavior to a relatively satisfactory degree over a narrow temperature range. In this work, however, the phase boundaries

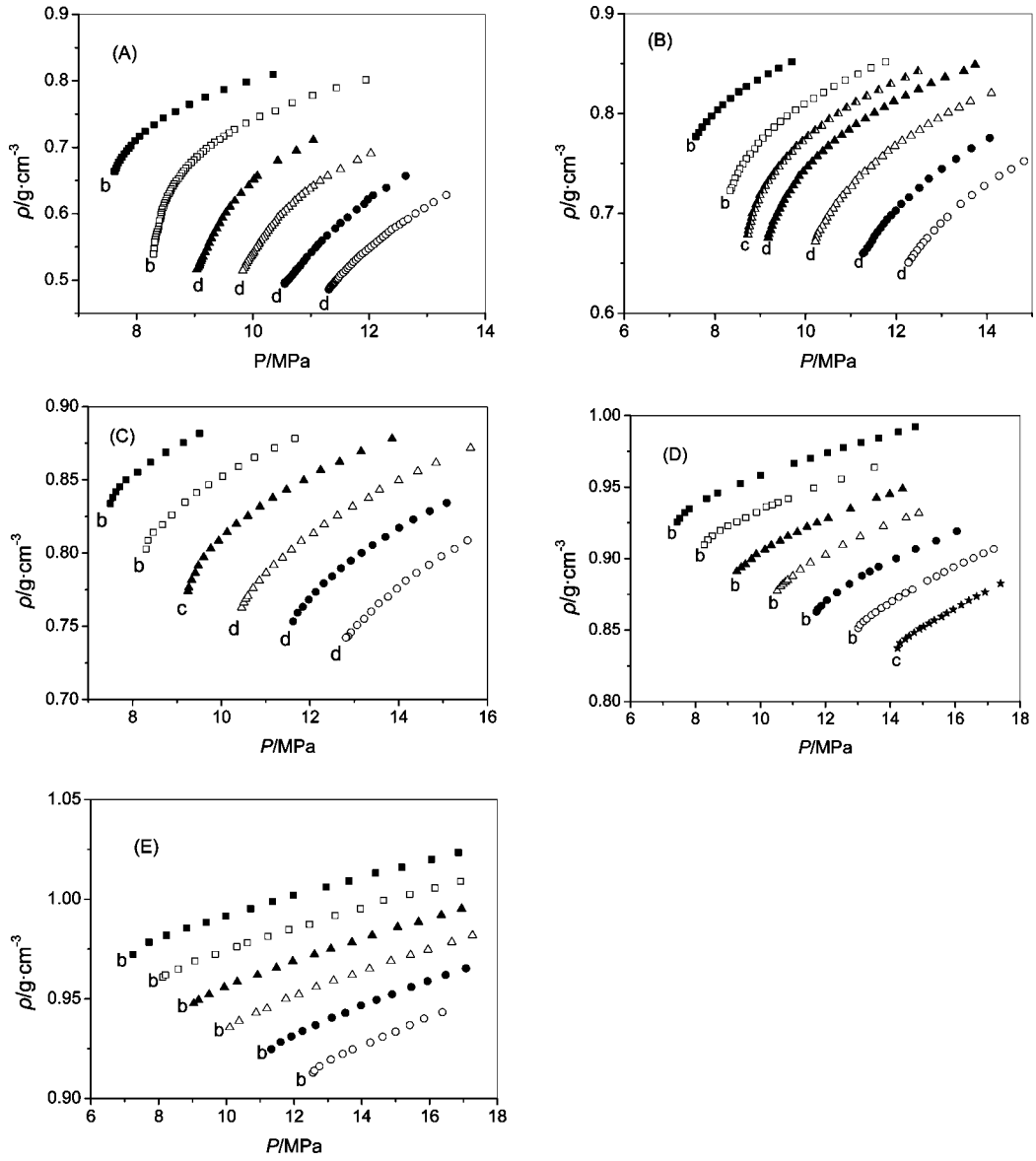

Figure 2. Dependence of the density of the CO_2 (1) + GVL (2) binary mixture on temperature and pressure in the critical region with different compositions: (A), $x_2 = 0.010$; (B), $x_2 = 0.025$; (C), $x_2 = 0.050$; (D), $x_2 = 0.100$; (E), $x_2 = 0.150$. Temperatures are labeled as follows: ■, $T = 308.2$ K; □, $T = 313.2$ K; ▲, $T = 316.2$ K; ▲, $T = 318.0$ K; △, $T = 322.9$ K; ●, $T = 327.9$ K; ○, $T = 332.9$ K; ★, $T = 337.9$ K.

Table 2. Densities of CO_2 (x_1) and GVL (x_2) Mixtures under Different Conditions

P/MPa	ρ/g·cm^{-3}	P/MPa	ρ/g·cm^{-3}	P/MPa	ρ/g·cm^{-3}	P/MPa	ρ/g·cm^{-3}	P/MPa	ρ/g·cm^{-3}
T = 308.2 K		T = 313.2 K		T = 318.0 K		T = 322.9 K		T = 327.9 K	
x_2 = 0.010		x_2 = 0.010		x_2 = 0.010		x_2 = 0.010		x_2 = 0.010	
7.62[b]	0.663[b]	8.29[b]	0.539[b]	9.04[d]	0.516[d]	9.83[d]	0.514[d]	10.55[d]	0.496[d]
7.63	0.665	8.30	0.547	9.06	0.519	9.85	0.518	10.57	0.497
7.65	0.669	8.31	0.557	9.08	0.522	9.87	0.521	10.60	0.500
7.67	0.673	8.32	0.561	9.09	0.525	9.89	0.526	10.63	0.502
7.69	0.677	8.33	0.565	9.11	0.529	9.92	0.529	10.66	0.505
7.72	0.681	8.34	0.568	9.12	0.532	9.94	0.532	10.69	0.509
7.75	0.685	8.35	0.572	9.14	0.535	9.96	0.535	10.72	0.511
7.79	0.690	8.37	0.576	9.18	0.542	9.98	0.539	10.74	0.514
7.83	0.694	8.38	0.581	9.22	0.549	10.00	0.540	10.77	0.517
7.87	0.698	8.39	0.589	9.25	0.556	10.02	0.542	10.82	0.522
7.91	0.703	8.41	0.592	9.29	0.563	10.05	0.547	10.88	0.529
7.97	0.710	8.42	0.596	9.33	0.570	10.08	0.550	10.93	0.535
8.05	0.717	8.43	0.602	9.38	0.578	10.10	0.554	11.01	0.542
8.15	0.724	8.44	0.606	9.43	0.586	10.11	0.556	11.08	0.549
8.30	0.734	8.46	0.609	9.48	0.593	10.14	0.559	11.13	0.554
8.46	0.744	8.47	0.612	9.54	0.602	10.17	0.563	11.19	0.559
8.67	0.754	8.48	0.616	9.61	0.611	10.20	0.566	11.28	0.567
8.91	0.765	8.50	0.619	9.69	0.619	10.23	0.576	11.42	0.578
9.18	0.775	8.52	0.623	9.80	0.631	10.26	0.574	11.51	0.586
9.50	0.787	8.53	0.627	9.93	0.642	10.29	0.578	11.63	0.594
9.89	0.798	8.56	0.630	10.02	0.652	10.33	0.582	11.79	0.606
10.35	0.810	8.58	0.634	10.08	0.657	10.37	0.586	11.92	0.615
		8.60	0.638	10.75	0.695	10.40	0.590	11.98	0.621
		8.63	0.641	11.04	0.711	10.43	0.594	12.07	0.628
		8.65	0.645			10.47	0.598	12.30	0.639
		8.68	0.649			10.52	0.602	12.63	0.657
		8.72	0.653			10.57	0.606		
		8.75	0.657			10.62	0.610		
		8.78	0.661			10.68	0.615		
		8.81	0.665			10.72	0.619		
		8.85	0.669			10.78	0.624		
		8.89	0.673			10.84	0.629		
		8.94	0.677			10.90	0.633		
		8.99	0.681			10.98	0.638		
		9.04	0.686			11.04	0.641		
		9.10	0.690			11.16	0.650		
		9.15	0.694			11.29	0.657		
		9.20	0.698			11.51	0.667		
		9.28	0.703			11.80	0.681		
		9.34	0.708			12.03	0.691		
		9.43	0.712						
		9.50	0.717						
		9.59	0.721						
		9.68	0.727						
		9.88	0.736						
		10.12	0.746						
		10.39	0.755						
		10.68	0.767						
		11.03	0.778						
		11.44	0.789						
		11.95	0.802						
T = 332.9 K		T = 308.2 K		T = 313.2 K		T = 316.2 K		T = 318.0 K	
x_2 = 0.010		x_2 = 0.025		x_2 = 0.025		x_2 = 0.025		x_2 = 0.025	
11.31[d]	0.486[d]	7.58[b]	0.777[b]	8.34[b]	0.723[b]	8.73[c]	0.679[c]	9.18[d]	0.677[d]
11.32	0.487	7.64	0.781	8.37	0.726	8.74	0.683	9.19	0.680
11.33	0.488	7.72	0.786	8.41	0.730	8.76	0.687	9.23	0.683
11.34	0.490	7.82	0.792	8.45	0.736	8.79	0.692	9.26	0.688
11.35	0.491	7.93	0.798	8.51	0.740	8.81	0.696	9.29	0.692
11.37	0.493	8.06	0.804	8.55	0.745	8.83	0.700	9.34	0.696
11.38	0.494	8.17	0.809	8.62	0.750	8.88	0.704	9.38	0.700
11.40	0.496	8.35	0.815	8.70	0.755	8.91	0.709	9.43	0.705
11.41	0.497	8.53	0.822	8.78	0.760	8.96	0.713	9.48	0.709
11.42	0.498	8.70	0.827	8.88	0.765	8.99	0.718	9.53	0.714
11.44	0.500	8.94	0.833	8.96	0.771	9.06	0.723	9.59	0.718
11.45	0.501	9.18	0.840	9.06	0.775	9.11	0.728	9.66	0.723
11.47	0.503	9.41	0.845	9.18	0.781	9.18	0.732	9.73	0.728
11.49	0.506	9.70	0.852	9.31	0.786	9.25	0.737	9.80	0.732
11.52	0.509			9.45	0.792	9.32	0.742	9.86	0.737
11.56	0.511			9.59	0.798	9.41	0.747	9.95	0.742
11.60	0.515			9.78	0.803	9.50	0.752	10.05	0.747
11.63	0.518			9.97	0.810	9.59	0.758	10.15	0.752
11.66	0.521			10.18	0.815	9.70	0.762	10.26	0.757

Table 2 Continued

P/MPa	ρ/g·cm^{-3}	P/MPa	ρ/g·cm^{-3}	P/MPa	ρ/g·cm^{-3}	P/MPa	ρ/g·cm^{-3}	P/MPa	ρ/g·cm^{-3}
T = 332.9 K		T = 308.2 K		T = 313.2 K		T = 316.2 K		T = 318.0 K	
x_2 = 0.010		x_2 = 0.025		x_2 = 0.025		x_2 = 0.025		x_2 = 0.025	
11.70	0.524			10.40	0.821	9.80	0.768	10.38	0.762
11.73	0.527			10.63	0.827	9.93	0.772	10.50	0.768
11.77	0.531			10.88	0.833	10.06	0.778	10.64	0.773
11.81	0.534			11.16	0.840	10.21	0.783	10.80	0.779
11.85	0.537			11.45	0.846	10.36	0.788	10.96	0.784
11.89	0.540			11.77	0.852	10.52	0.794	11.12	0.789
11.94	0.543					10.72	0.800	11.32	0.795
11.99	0.547					10.91	0.806	11.52	0.801
12.04	0.551					11.11	0.812	11.74	0.806
12.09	0.554					11.35	0.818	11.95	0.813
12.14	0.558					11.61	0.824	12.21	0.818
12.19	0.561					11.88	0.830	12.49	0.824
12.24	0.565					12.20	0.836	12.77	0.830
12.29	0.569					12.48	0.842	13.08	0.836
12.34	0.573							13.49	0.843
12.39	0.576							13.74	0.849
12.46	0.580								
12.53	0.584								
12.59	0.588								
12.67	0.592								
12.80	0.600								
12.95	0.608								
13.11	0.617								
13.33	0.628								
T = 322.9 K		T = 327.9 K		T = 332.8 K		T = 308.2 K		T = 313.2 K	
x_2 = 0.025		x_2 = 0.025		x_2 = 0.025		x_2 = 0.050		x_2 = 0.050	
10.22[d]	0.672[d]	11.27[d]	0.660[d]	12.26[d]	0.649[d]	7.50[b]	0.834[b]	8.30[b]	0.803[b]
10.23	0.673	11.30	0.661	12.27	0.651	7.56	0.838	8.34	0.809
10.24	0.675	11.36	0.665	12.28	0.652	7.63	0.842	8.46	0.814
10.27	0.679	11.42	0.669	12.34	0.655	7.71	0.845	8.67	0.820
10.31	0.683	11.48	0.673	12.39	0.659	7.85	0.850	8.88	0.826
10.37	0.687	11.52	0.677	12.46	0.663	8.11	0.855	9.18	0.835
10.44	0.692	11.59	0.682	12.53	0.667	8.40	0.862	9.44	0.841
10.47	0.696	11.66	0.686	12.60	0.671	8.75	0.869	9.71	0.847
10.54	0.701	11.73	0.690	12.68	0.675	9.14	0.875	10.03	0.852
10.61	0.705	11.80	0.694	12.84	0.683	9.51	0.881	10.39	0.859
10.67	0.710	11.89	0.698	12.98	0.690			10.75	0.865
10.75	0.714	11.99	0.703	13.13	0.696			11.20	0.872
10.82	0.718	12.11	0.709	13.42	0.710			11.66	0.878
10.91	0.723	12.28	0.716	13.67	0.718				
11.02	0.727	12.51	0.726	13.94	0.728				
11.09	0.732	12.72	0.735	14.27	0.738				
11.19	0.737	13.01	0.745	14.54	0.744				
11.31	0.742	13.32	0.755	14.82	0.752				
11.45	0.747	13.66	0.765	15.19	0.761				
11.54	0.751	14.06	0.776						
11.70	0.757								
11.82	0.763								
11.97	0.768								
12.13	0.773								
12.33	0.778								
12.52	0.784								
12.71	0.790								
12.92	0.795								
13.15	0.801								
13.39	0.806								
13.64	0.812								
14.10	0.821								
T = 318.0 K		T = 322.9 K		T = 327.9 K		T = 332.9		T = 308.2 K	
x_2 = 0.050		x_2 = 0.050		x_2 = 0.050		x_2 = 0.050		x_2 = 0.100	
9.25[c]	0.774[c]	10.46[d]	0.763[d]	11.62[d]	0.753[d]	12.81[d]	0.742[d]	7.43[b]	0.926[b]
9.27	0.776	10.51	0.766	11.72	0.759	12.82	0.743	7.52	0.928
9.33	0.782	10.55	0.769	11.84	0.763	12.86	0.743	7.67	0.932
9.41	0.787	10.60	0.771	11.97	0.768	12.92	0.746	7.81	0.935
9.48	0.792	10.72	0.776	12.13	0.774	13.06	0.751	8.34	0.942
9.60	0.797	10.86	0.781	12.31	0.779	13.22	0.755	8.68	0.946
9.76	0.803	11.01	0.787	12.50	0.784	13.38	0.760	9.38	0.953
9.94	0.809	11.18	0.792	12.70	0.790	13.55	0.766	10.00	0.958
10.13	0.814	11.38	0.797	12.92	0.795	13.76	0.770	11.04	0.967
10.34	0.820	11.58	0.803	13.16	0.800	13.96	0.776	11.55	0.970
10.60	0.825	11.80	0.808	13.41	0.805	14.16	0.781	12.07	0.974
10.87	0.832	12.08	0.814	13.70	0.811	14.40	0.786	12.55	0.978

Table 2 Continued

P/MPa	ρ/g·cm^{-3}	P/MPa	ρ/g·cm^{-3}	P/MPa	ρ/g·cm^{-3}	P/MPa	ρ/g·cm^{-3}	P/MPa	ρ/g·cm^{-3}
T = 318.0 K		T = 322.9 K		T = 327.9 K		T = 332.9		T = 308.2 K	
x_2 = 0.050		x_2 = 0.050		x_2 = 0.050		x_2 = 0.050		x_2 = 0.100	
11.16	0.838	12.32	0.820	14.01	0.817	14.68	0.792	13.11	0.981
11.47	0.843	12.62	0.826	14.33	0.823	14.96	0.798	13.64	0.984
11.86	0.850	12.96	0.832	14.70	0.829	15.26	0.803	14.25	0.989
12.24	0.857	13.32	0.838	15.08	0.835	15.55	0.809	14.77	0.992
12.67	0.862	13.57	0.843						
13.15	0.869	14.00	0.850						
13.85	0.878	14.43	0.856						
		14.84	0.862						
		15.62	0.872						
T = 313.2 K		T = 318.0 K		T = 322.9 K		T = 327.9 K		T = 332.9 K	
x_2 = 0.100		x_2 = 0.100		x_2 = 0.100		x_2 = 0.100		x_2 = 0.100	
8.27[b]	0.910[b]	9.28[b]	0.891 [b]	10.52[b]	0.877 [b]	11.73[b]	0.863 [b]	13.01[b]	0.851 [b]
8.38	0.913	9.41	0.894	10.63	0.881	11.74	0.864	13.07	0.854
8.52	0.916	9.54	0.896	10.70	0.882	11.77	0.865	13.17	0.856
8.76	0.920	9.73	0.900	10.77	0.884	11.88	0.867	13.27	0.858
9.00	0.923	9.88	0.903	10.84	0.885	12.05	0.871	13.42	0.861
9.28	0.926	10.14	0.906	11.00	0.888	12.36	0.876	13.55	0.863
9.55	0.929	10.34	0.909	11.23	0.892	12.74	0.882	13.73	0.865
9.88	0.932	10.61	0.912	11.54	0.897	13.13	0.888	13.89	0.867
10.18	0.936	10.85	0.916	12.01	0.903	13.37	0.891	14.06	0.870
10.37	0.938	11.14	0.919	12.54	0.910	13.64	0.894	14.26	0.873
10.54	0.939	11.44	0.922	13.08	0.915	14.18	0.900	14.47	0.876
10.86	0.942	11.75	0.925	13.79	0.923	14.78	0.907	14.68	0.878
11.64	0.949	12.09	0.928	14.49	0.929	15.41	0.913	15.14	0.884
12.49	0.956	12.78	0.935	14.88	0.932	16.05	0.919	15.42	0.888
13.51	0.964	13.58	0.943					15.66	0.891
		13.99	0.945					15.95	0.894
		14.38	0.949					16.26	0.897
								16.56	0.900
								16.87	0.904
								17.19	0.907
T = 337.9 K		T = 308.2 K		T = 313.2 K		T = 318.0 K		T = 322.9 K	
x_2 = 0.100		x_2 = 0.150		x_2 = 0.150		x_2 = 0.150		x_2 = 0.150	
14.23[c]	0.837 [c]	7.25[b]	0.972 [b]	8.12[b]	0.961[b]	9.04[b]	0.948[b]	10.10[b]	0.936[b]
14.31	0.841	7.71	0.979	8.20	0.962	9.18	0.949	10.38	0.939
14.47	0.844	8.23	0.982	8.58	0.965	9.49	0.952	10.88	0.943
14.58	0.846	8.83	0.985	9.07	0.969	9.94	0.956	11.20	0.945
14.74	0.848	9.40	0.988	9.67	0.972	10.32	0.959	11.76	0.950
14.90	0.851	9.98	0.991	10.31	0.976	10.92	0.962	12.14	0.952
15.02	0.852	10.72	0.995	10.62	0.978	11.48	0.966	12.66	0.956
15.20	0.855	11.36	0.999	11.23	0.981	11.96	0.969	13.17	0.959
15.36	0.857	11.98	1.002	11.85	0.985	12.60	0.972	13.72	0.962
15.58	0.859	12.95	1.006	12.46	0.987	13.09	0.975	14.23	0.965
15.74	0.862	13.62	1.009	13.22	0.992	13.71	0.978	14.86	0.969
15.94	0.864	14.41	1.013	13.96	0.995	14.31	0.982	15.44	0.972
16.19	0.868	15.18	1.016	14.65	0.999	15.06	0.986	15.96	0.975
16.42	0.871	16.06	1.020	15.42	1.002	15.68	0.989	16.66	0.979
16.66	0.874	16.85	1.023	16.16	1.006	16.35	0.992	17.27	0.982
16.92	0.877			16.92	1.009	16.95	0.995		
17.40	0.883								
T = 327.9 K		T = 332.9 K							
x_2 = 0.150		x_2 = 0.150							
11.33[b]	0.925[b]	12.56[b]	0.913[b]						
11.60	0.928	12.60	0.914						
11.92	0.931	12.75	0.916						
12.25	0.934	13.09	0.919						
12.64	0.937	13.44	0.922						
13.12	0.941	13.73	0.925						
13.52	0.943	14.25	0.928						
13.98	0.947	14.62	0.931						
14.44	0.949	15.00	0.933						
14.90	0.952	15.42	0.937						
15.46	0.956	15.84	0.940						
15.94	0.959	16.38	0.943						
16.48	0.962								
17.08	0.965								

[b] : bubble point. [c] : critical point. [d] : dew point.

of binary mixtures were measured over a very wide range of temperatures. Therefore, two interaction parameters are needed to calculate the phase boundaries. The k_{ij} and l_{ij} values for the binary mixtures involved in this work are shown in Table 3;

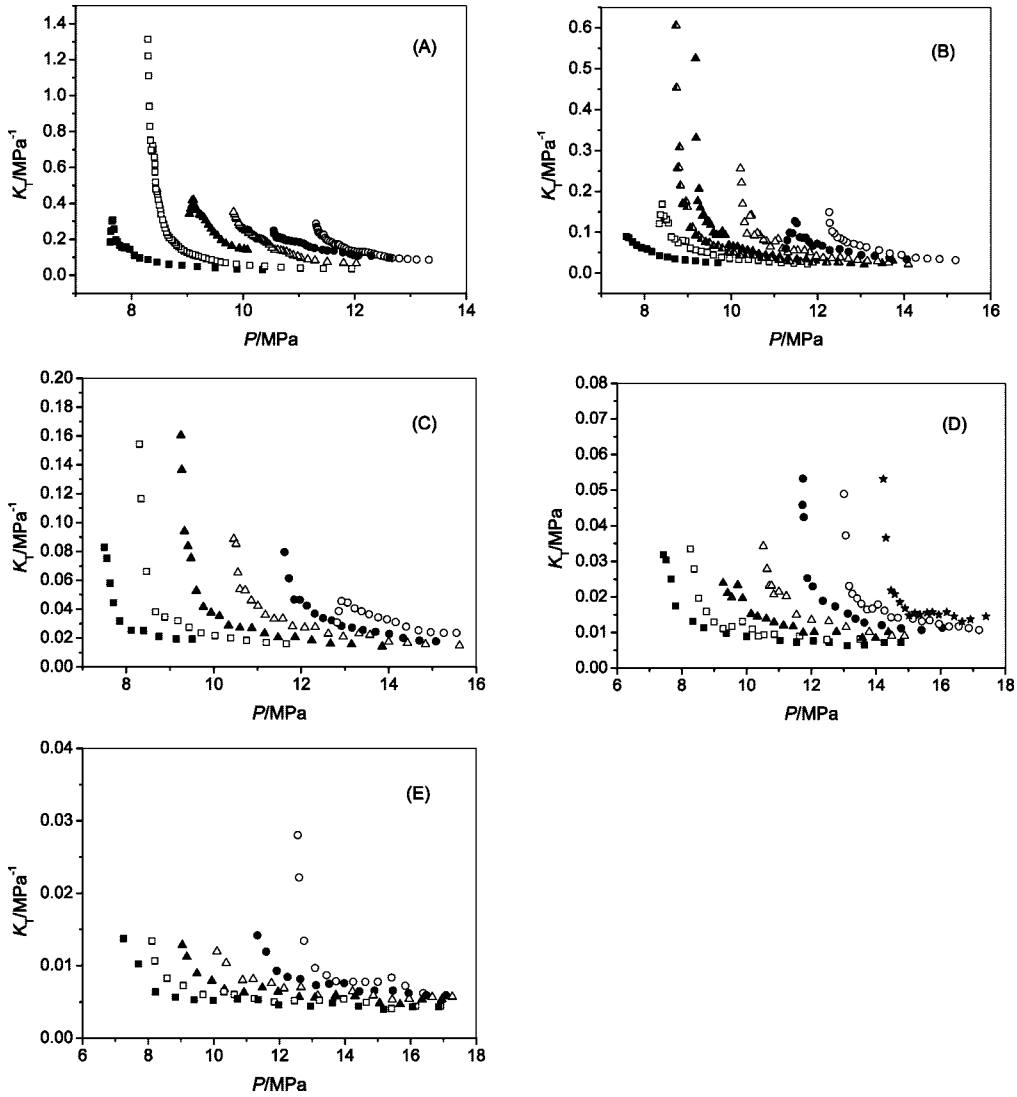

Figure 3. Dependence of the isothermal compressibility (K_T) of the CO_2 (1) + GVL (2) binary mixture on temperature and pressure with different compositions: (A), $x_2 = 0.010$; (B), $x_2 = 0.025$; (C), $x_2 = 0.050$; (D), $x_2 = 0.100$; (E), $x_2 = 0.150$. Temperatures are labeled as follows: ■, $T = 308.2$ K; □, $T = 313.2$ K; ▲, $T = 316.2$ K; ▲, $T = 318.0$ K; △, $T = 322.9$ K; ●, $T = 327.9$ K; ○, $T = 332.9$ K; ★, $T = 337.9$ K.

Table 3. Pure Component Parameters and Interaction Parameters Used in the Peng−Robinson Equation of State and Corresponding Values of the Root-Mean-Square Relative Deviation (RMSRD) for CO_2 + GVL System

components	T_c/K	P_c/MPa	ω	k_{12}	l_{12}	RMSRD
CO_2	304.3	7.38	0.225	0.00	−0.03	3.85
GVL	721.6[a]	4.09[a]	0.367[a]			

[a] Calculated using the method reported by Joback and Reid.[12]

they were obtained by minimizing the following objective function (OF).

$$\mathrm{OF} = \sqrt{\frac{1}{n}\sum_{i=1}^{n}\left(\frac{\xi^{\mathrm{exptl}} - \xi^{\mathrm{calcd}}}{\xi^{\mathrm{exptl}}}\right)^2} \qquad (9)$$

where n is the number of experimental points and ξ^{exptl} and ξ^{calcd} are the experimental and the calculated temperature or pressure at each phase transition point, respectively.

The root-mean-squared relative deviation (RMSRD) of this calculation was defined as follows

$$\mathrm{RMSRD} = \sqrt{\frac{1}{n}\sum_{i=1}^{n}\left(\frac{\xi^{\mathrm{exptl}} - \xi^{\mathrm{calcd}}}{\xi^{\mathrm{exptl}}}\right)^2} \cdot 100\ \% \qquad (10)$$

The corresponding value of RMSRD is also shown in Table 3.

On the basis of the physical properties and the two binary interaction parameters, the PR EOS was used to correlate the phase behavior of the CO_2 and GVL binary system as shown in Figure 1. It can be seen from the figures that the PR EOS can correlate the phase boundary of CO_2 and GVL to a satisfactory degree from (308.2 to 550.2) K and concentrations of GVL from (0.01 to 0.15) in mole fraction.

Conclusion

The phase behavior of the CO_2 and GVL binary system has been determined at different temperatures and pressures with GVL concentrations from (0.01 to 0.15) in mole fraction. The density of the binary mixture was also measured at fixed composition and fixed temperature. The isothermal compressibility (K_T) was calculated from the density of the binary

mixture. The Peng−Robinson equation of state was used to correlate the experimental data. The results reveal that the density is sensitive to the pressure near the critical of the mixtures. When the pressure is much higher than the phase separation pressure or the composition is far from the critical composition, K_T is very small, and the effect of pressure on K_T is very limited. The phase boundary data CO_2 + GVL can be correlated well by the Peng−Robinson equation of state (PR EOS) with two interaction parameters.

Acknowledgment

We thank Dr. J. Ke, Prof. M. W. George, Prof. M. Nunes da Ponte, Dr. P. License, Mr. M. Guyler, Mr. R. Wilson, and Mr. P. Fields for their help.

Literature Cited

(1) Horvath, I. T.; Mehdi, H.; Fabos, V.; Boda, L.; Mika, L. T. γ-Valerolactone−a Sustainable Liquid for Energy and Carbon-Based Chemicals. *Green Chem.* **2008**, *20*, 238–242.

(2) Lourvanij, K.; Rorrer, G. L. Dehydration of Glucose to Organic Acids in Microporous Pillared Clay Catalysts. *Appl. Catal., A* **1994**, *109*, 147–165.

(3) Manzer, L. E. Production of 5-Methylbutyrolactone from Levulinic Acid. US Pat., 20030055270, 2003.

(4) Bourne, R.; Stevens, J. G.; Ke, J.; Poliakoff, M. Maximising Opportunities in Supercritical Chemistry: The Continuous Conversion of Levulinic Acid to γ-Valerolactone in CO_2. *Chem. Commun.* **2007**, 4632–4634.

(5) Manzer, L. E.; Hutchenson, K. W. Production of 5-methyl-dihydro-furan-2-one from levulinic acid in supercritical media. US Pat., 20040254384, 2004.

(6) Wang, B.; Wu, W. Z.; Chen, J. W.; Han, B. X.; Zhang, Z. F.; Shen, D.; Zhang, R. Phase Behavior, Densities and Isothermal Compressibility of CO_2 + Ethanol + Dichloromethane Ternary System in Different Phase Regions. *J. Chem. Eng. Data* **2005**, *50*, 1153–1156.

(7) Chen, J. W.; Wu, W. Z.; Han, B. X.; Gao, L.; Mu, T. C.; Liu, Z. M.; Jiang, T.; Du, J. M. Phase Behaviors and Densities and Isothermal Compressibility of CO_2+n-Pentane and CO_2 + Acetone Systems in Various Phase Regions. *J. Chem. Eng. Data* **2003**, *48*, 1544–1548.

(8) Wu, W. Z.; Ke, J.; Poliakoff, M. Phase Boundaries of CO_2 + Toluene, CO_2 + Acetone, and CO_2 + Ethanol at High Temperatures and High Pressures. *J. Chem. Eng. Data* **2006**, *51*, 1398–1403.

(9) Wu, W. Z.; Ke, J.; Poliakoff, M. A New Design of Fiber Optic Reflectometer for Determining the Phase Boundary of Multi-Component Fluid Mixtures at High Pressures and High Temperatures. *Rev. Sci. Instrum.* **2006**, *77*, 1–4, 023903.

(10) Stradi, B. A.; Kohn, J. P.; Stadtherr, M. A.; Brennecke, J. F. Phase Behavior of the Reactants, Products and Catalysts involved in the Allylic Epoxidation of Trans-2-Hexen-1-ol to (2R,3R)- (+)-3- Propyloxiranemethanol in High Pressure Carbon Dioxide. *J. Supercrit. Fluids* **1998**, *12*, 109–122.

(11) Peng, D. Y.; Robinson, D. B. A New Two-Constant Equation of State. *Ind. Eng. Chem. Fundam.* **1976**, *15*, 59–64.

(12) Joback, K. G.; Reid, R. C. Estimation of Pure-Component Properties from Group-Contribution. *Chem. Eng. Commun.* **1987**, *57*, 233–243.

Received for review October 20, 2008. Accepted November 17, 2008. This work was supported by the National Natural Science Foundation of China (20776004) and Beijing Natural Science Foundation (2082017). We thank EPSRC Grants (GR/R02863 and GR/S87409) and the Marie Curie Research Training Network SuperGreenChem (MRTN-CT-2004-504005) for financial support.

JE8007759